

Influence of Methanol on the Dynamics of the Retention and Release of Cyprodinil by an Agricultural Soil

JOSÉ EUGENIO LÓPEZ-PERIAGO,[†] MANUEL ARIAS-ESTÉVEZ,[†]
 BENEDICTO SOTO-GONZÁLEZ,[†] SARA TRELLES-REINOSO,[†] AND
 JESÚS SIMAL-GÁNDARA^{*,‡}

Soil and Agricultural Science Group, Plant Biology and Soil Science Department, and Nutrition and Bromatology Group, Analytical and Food Chemistry Department, Faculty of Food Science and Technology, University of Vigo, Ourense Campus, 32004 Ourense, Spain

The influence of methanol on the adsorption of the fungicide cyprodinil by a crop soil was studied by equilibrium measurements and by determining the retention–release dynamics in a continuous stirred flow tank reactor (CSTR). Equilibrium measurements showed the effective coefficient of partition of cyprodinil between soil and solution, K_{dc} , decreases linearly as the concentration of methanol in the solution increases until a percentage of 20% is reached. In CSTR experiments, the retention of cyprodinil was found to be almost reversible; up to a 95% of the fungicide was desorbed. The retention–release dynamics showed biphasic behavior and was partially controlled by diffusion. This behavior was reproduced by a model of diffusion into micropores identifying the soil particles as spheres and taking into account both intraparticle nonlinear adsorption and nonlinear adsorption at external surfaces. In all cases, the sorption kinetics was not the limiting step. The main effect of methanol in the retention–release dynamics ended up being based on the changes produced in the adsorption equilibrium. Methanol also increased the effective diffusion coefficient and decreased the mass transfer coefficient. The optimized Freundlich's isotherm coefficients for <5% methanol were lower than those obtained from the batch experiments.

KEYWORDS: Cyprodinil; adsorption; kinetics; stirred flow

INTRODUCTION

Pesticides can have marked effects on soil microbiota and, potentially, on organisms in any waters they may reach. The magnitude of such effects depends, among other things, on the processes that govern their mobility in soil. The mobility of moderately hydrophobic pesticides, like that of hydrophobic compounds in general, depends to a significant extent on hydrophobic interactions mediating their adsorption onto soil particles (1, 2) and can be affected by any cosolvents that have been introduced, accidentally or intentionally, into the soil solution (3). Among other causes of the presence of cosolvents in the soil solution are their use as components of formulations used in agriculture and their use to solubilize poorly soluble substances in gaining access to a wider concentration range in experiments aimed at determining the adsorption isotherms of such substances.

There have accordingly been numerous studies of the influence of cosolvents on various aspects of the mobility of organic contaminants (3–8). Haws and co-workers (9) indicate that cosolvents can increase the solubility of nonpolar pesticide solutes by reducing the polarity of the aqueous mixture.

According to them, cosolvents might also compete for sorption sites, thereby increasing the aqueous concentrations and thus the overall bioavailability of a contaminant of interest. Other authors (10) have reviewed different hypotheses and attributed cosolvent effects to changes in the hydrophobic driving force for the formation of the pesticide complex, changes in the solvophobic characteristics of the medium, or a decrease in the stoichiometric equilibrium with the addition of organic cosolvents. For the ionizable organic pesticides, all these changes affect the acid dissociation constant and therefore the distribution between neutral and ionized species (2).

The stirred flow technique in a continuously stirred tank reactor (CSTR) (11, 12) has been used for studying adsorption kinetics of metals in soils (13) and recently used in studies of the sorption kinetics of organic compounds (14, 15). This technique is particularly appropriate for studying pesticide retention dynamics on a relatively short time scale (i.e., those that are typical of storm events) (16) and has advantages over both column experiments (vigorous stirring minimizes diffusion problems) and batch experiments (the continuous injection or withdrawal of pesticide minimizes changes in its concentration).

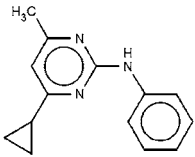
Cyprodinil (4-cyclopropyl-6-methyl-*N*-phenylpyrimidine) (17) (Table 1) is a systemic fungicide recommended for prevention and treatment of various rots of fungal origin that can affect

* To whom correspondence should be addressed. E-mail: jsimal@uvigo.es.

[†] Plant Biology and Soil Science Department.

[‡] Analytical and Food Chemistry Department.

Table 1. Characteristics of Cyprodinil^a

Chemical family	Aniline pyrimidine
Structural formula	
CAS number	121552-61-2
pKa	4.44
Solubility (mg L ⁻¹ , 25 °C)	In water 13 (at pH 7.0) 20 (at pH=5) In methanol 150
Koc (L kg ⁻¹)	2219
Octanol/water partition coefficient at 25 °C	log Pow = 3.9 at pH 5.0 log Pow = 4.0 at pH 7.0
Initial half-life (incubated for 21 d in sandy loam soil, at 30-60% field capacity moisture, 25°C, pH 5.2).	22-30 d
Final half-life (incubation time: 363 d)	433-600 d

^aData from ref 17.

fruit plants. Because of its recent introduction, there is less information about the dynamics of cyprodinil in the soil than there is for older pesticides. The sorption characteristics of reagent-grade cyprodinil in vineyard soils in the absence of cosolvents have been reported by us elsewhere (18). In the study described here, we investigated the influence of methanol on the sorption of cyprodinil in an agricultural soil, using batch experiments to characterize equilibria and CSTR experiments to characterize the retention–release dynamics.

EXPERIMENTAL PROCEDURES

Study Soil. A sample of the top 20 cm of a Typic haplumbrept (19), sandy loam textured soil developed from alluvial sediments was taken in an agricultural field near Ourense, Spain (42° 07' 13.45" N, 7° 42' 7.15" W). The sample was air-dried, and the fraction smaller than 2 mm was obtained by sieving and preconditioned as described by Strawn and Sparks to remove organic components to which poor reproducibility of adsorption has been attributed (20). Analyses of five replicate subsamples of the resulting fraction showed it to be 8% clay, 25% silt, and 67% sand (geometric mean diameter of 0.023 cm and geometric standard deviation of 0.96 cm) and to have pH values of 5.5 in water and 4.8 in KCl, an organic carbon content of 1.8%, and a cation exchange capacity (CEC) of 4.7 cmol(+)/kg when buffered at pH 7.

Determination of the Amount of Cyprodinil. All experiments were performed using 99% pure analysis grade cyprodinil from Riedel-de Haën (Seelze, Germany).

Cyprodinil in soil solutions was identified and quantified by HPLC using Thermo Separation Products equipment comprising a P2000 binary pump, a degassing unit, an AS1000 automatic injector, a 100 μ L loop, and a UVIS20 UV detector operating at 270 nm. A 150 mm \times 4.6 mm Waters Symmetry 5 μ m C18 column was used with a 50 mm \times 4.6 mm Pelliguard LC-18 40 μ m guard column. Samples (100

μ L) were run at room temperature with a 1 mL/min flow of a 7:3 acetonitrile/water mixture (water purified with a MilliQ apparatus). Data were acquired and processed using ChromCard 2.17.

Batch Experiments. Sorption equilibria were investigated in a series of triplicate batch experiments. In each replicate, 2 g of preconditioned soil was placed in a 30 mL glass tube and suspended in 16, 18, 19, or 19.76 mL of 0.01 M CaCl₂. The volume was increased to 20 mL with methanol (giving methanol fractions f_c of 20, 10, 5, and 1.2%, respectively), and the tube was closed with a Teflon stopper and shaken at 200 rpm for 12 h at 25 \pm 1 °C. The suspension was then treated with 40, 80, 120, 160, 200, or 240 μ L of a 1000 mg/L solution of cyprodinil in methanol (additions were made with a Hamilton syringe), giving cyprodinil concentrations of 2, 4, 6, 8, 10, and 12 mg/L, respectively. After being shaken for a further 12 h, the suspension was centrifuged for 30 min at 536g, the amount of cyprodinil in the supernatant was determined, and the amount of cyprodinil adsorbed by the soil sample was calculated by difference. For each methanol mixture, triplicate tests without soil were made to take into account the effects of degradation in the methanol/water phase and adsorption on the tube walls. Cyprodinil degradation on the experiment time scale is rejectable (Table 1).

The smallest methanol fraction that was used, 1.2%, was that which in preliminary experiments had proved to allow least dissolution of sufficient cyprodinil to attain the highest cyprodinil concentration required, 12 mg/L.

Stirred-Flow Experiments. Apparatus and Calibration. Stirred-flow experiments were carried out using a stainless steel reactor with a horizontal inlet at the bottom, an outlet through the top, and an internal volume of 5.6 cm³. On the inner side of the inlet and outlet, fritted stainless steel filters 10 mm in diameter with 0.2 μ m pores were installed so that the soil sample was kept in the reactor. Influent was pumped through the reactor by a Waters 510 HPLC pump. A Rheodyne 5011 valve between the pump and the influent solution tanks allowed switching between influents without cyprodinil ["cyprodinil-free influents", mixtures of methanol and 0.05 M CaCl₂ (pH 6.0) with the same methanol fractions f_c as in the batch experiments] and influents containing cyprodinil ("cyprodinil-bearing influents", 4 mg/L solutions of cyprodinil in the cyprodinil-free influent mixtures). The mixture inside the reactor was stirred at 400 rpm with a PTFE-coated magnetic stirring bar. The concentration of cyprodinil in the effluent was determined using a Gilson 118 UV–vis detector operating at 270 nm connected to a ChromCard data acquisition system that collected data once per second; the detector was calibrated and the linearity of its response verified using solutions of cyprodinil in cyprodinil-free influent mixtures. Because of computational limitations, in analyses of these kinetic data, only the first of every 10 measurements was used.

Preliminary Experiments for Establishing the Experimental Conditions. Before using the equipment to characterize the cyprodinil retention dynamics, we performed experiments to check the efficiency of stirring in the reactor, to determine its effective volume, and to determine flow and reagent concentration conditions that were appropriate for the recording of kinetic data. These experiments are described in Results and Discussion.

Procedure. The soil fraction selected for the experiments was smaller than 0.5 mm (this fraction was the 90% of the <2 mm sample and had a geometric mean diameter of 0.01 cm). Experiments involved loading the reactor with a suspension of 0.75 g of such a soil fraction in the appropriate cyprodinil-free influent mixture, pumping that same cyprodinil-free influent through the reactor until the detector reading had stabilized, switching to the cyprodinil-bearing influent with the same f_c for 13 min (the retention stage), and finally switching back to the cyprodinil-free influent for passage of a further 45 reactor volumes (the release stage). The flow rate was 5 mL/min throughout, and all experiments were performed at 20 \pm 2 °C. Retention and release of cyprodinil were assessed from the recorded c_t data as described by Yin et al. (21).

RESULTS AND DISCUSSION

Batch Experiments. Increasing the methanol fraction (f_c) reduced the mass of cyprodinil adsorbed per unit weight of soil

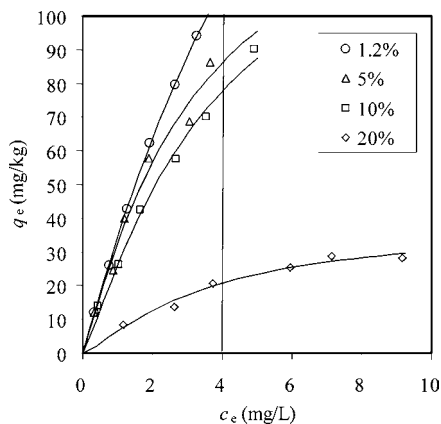


Figure 1. Observed relationship between soil cyprodinil content and the concentration of cyprodinil in solution at equilibrium (averages of three replicate experiments). Curves are fitted Freundlich isotherms. The vertical line indicates the influent concentration of cyprodinil in subsequent stirred-flow experiments.

Table 2. Freundlich Isotherm Parameters Obtained by Fitting the Isotherm Equation to the Equilibrium Data for Each Methanol Concentration (q_e and c_e), Together with the Corresponding Gross Partition Constants (K_{dc}) Calculated As Shown in eq 2

f_c (%)	K_F^a ($\text{mg}^{n-1} \text{L}^n \text{kg}^{-1}$)	n^a	r^2	K_{dc} (L/kg)
1.2	34.7 (2.1)	0.85 (0.04)	0.9984	30.5
5	32.5 (2.3)	0.74 (0.06)	0.9744	26.1
10	27.4 (2.2)	0.75 (0.05)	0.9977	22.1
20	9.07 (3.0)	0.55 (0.07)	0.9425	6.28

^a Standard deviations in parentheses.

at equilibrium, q_e (Figure 1). The relationship between q_e and c_e , the concentration of cyprodinil in solution at equilibrium, was satisfactorily described by Freundlich isotherms

$$q_e = K_F(c_e)^n \quad (1)$$

with the parameters K_F and n listed in Table 2. Increasing f_c caused the expected reduction in the affinity of cyprodinil for the soil, as reflected by the K_F , but this reduction was greater in the isotherm interval corresponding to the highest levels of cyprodinil. The reduction in n with regard to f_c shows that the effect of methanol on cyprodinil retention is also dependent on the isotherm region: the diminution in the affinity of cyprodinil for the soil is again greater in the isotherm interval corresponding to the highest levels of cyprodinil.

Determining, for each isotherm, the effective partition constant (K_{dc}) such that

$$\int_{c_1}^{c_2} K_{dc} c \, dc = \int_{c_1}^{c_2} K_F c^n \, dc \quad (2)$$

where $c_1 = 0$ mg/L and $c_2 = 4$ mg/L, shows that K_{dc} falls more rapidly with an increase in f_c in the region where $f_c > 10\%$ than in the region where $f_c < 10\%$ (Figure 2). These results are in good agreement with those of other authors (10): when $f_c < 20\%$, the solubility increase follows a linear relationship, but in the whole concentration interval (1–100%), the increase follows a log-linear relationship. Backward linear extrapolation estimates the theoretical effective partition constant in the absence of methanol, K_{dw} , to be 32.8 L/kg.

Stirred-Flow Experiments. Establishment of Experimental Conditions and Parameters. The effective volume of the reactor, V_e , was determined in an experiment in which the reactor held

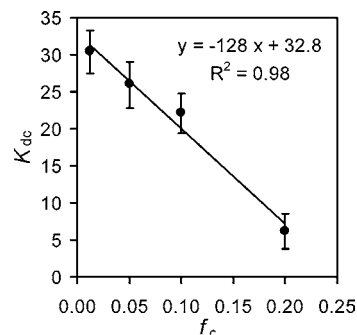


Figure 2. Relationship between K_{dc} (calculated as shown in eq 2) and the methanol content of the medium (vol %, f_c), together with the straight line fitted to the data for f_c values between 1.2 and 20% (—).

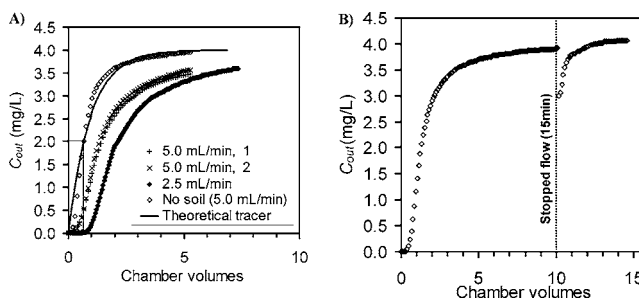


Figure 3. (A) Theoretical breakthrough curve $c(t)$ (eq 3) for a J of 5 mL/min and perfect mixing without adsorption, together with cyprodinil breakthrough data obtained with a J of 5 mL/min and no soil in the reactor (\diamond) or with 0.75 g of soil (two replicates, + and \times) or with a J of 2.5 mL/min and 0.75 g of soil in the reactor (\blacklozenge). (B) Cyprodinil breakthrough curve $c(t)$ obtained with 0.75 g of soil in the reactor with a J of 5.0 mL/min for 10 reactor volumes, 0 mL/min for 15 min, and finally a J of 5.0 mL/min for 5 reactor volumes.

no soil and the influent was switched at time zero between a cyprodinil-free influent and the corresponding cyprodinil-bearing influent; the value of V_e was obtained by fitting the equation

$$c_i = c_{in}[1 - \exp(-Jt/V_e)] \quad (3)$$

to the recorded c_i data, where c_i is the concentration of cyprodinil in the effluent at time step t_i , c_{in} is the concentration of cyprodinil in the influent (4 mg/L), and J is the flow rate (5 mL/min). Figure 3A shows the experimental data (\diamond) and the fitted curve (—), with Jt expressed as reaction chamber volumes. The good fit confirms that in the absence of soil the reactor behaved nearly as a perfect mixer. The value of V_e so obtained did not differ significantly from the physical volume of the reactor, 5.6 cm^3 . However, since the soil samples loaded into the reactor in subsequent experiments weighed 0.75 g (giving a solid concentration of 134 g/L) and the soil had a particle density of 2.6 g/cm^3 , the value used subsequently for V_e in experiments with soil was 5.3 cm^3 .

Loading the reactor with 0.75 g of soil shifted the c versus Jt curve reproducibly to the right, and halving the flow rate caused a further shift to the right. This behavior confirmed that the time scale of the retention of cyprodinil by the soil allowed investigation of the dynamics of this process with the chosen experimental conditions. Similarly, the drop in cyprodinil concentration in the effluent that occurred when the inflow was interrupted after passage of 10 reaction chamber volumes and restarted 15 min later (Figure 3B) confirmed that the retention process had not reached equilibrium at this time (11).

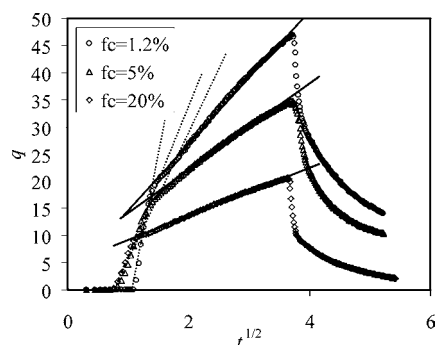


Figure 4. Dependence of soil cyprodinil content on the square root of time in stirred-flow experiments, for various methanol fractions f_c , together with straight lines fitted to the fast (···) and slow (—) adsorption phases in each case.

Retention Dynamics. Retention dynamics was calculated from the recorded discrete $c_i = c(t_i)$ data correcting for nonideality of mixing as follows (21):

$$q_i = (V_e/m)(c_{i+1}^B - c_{i+1}^S) + (J\Delta t/m) \sum_{j=1}^i (c_j^B - c_j^S) \quad (4)$$

where q_i is the mass of cyprodinil retained per unit weight of soil by time i , m is the mass of soil (0.75 g), Δt is the time interval between measurements, and superscripts B and S indicate measurements in the absence and presence of soil, respectively. During an initial fast retention time lasting ~ 2 min ($Jt < \sim 2$ reactor volumes), q increased rapidly to values that ranged from 23 mg/kg with an f_c of 1.2% to 10 mg/kg with an f_c of 20.

In **Figure 4**, the dependence of soil cyprodinil content on the square root of time in stirred-flow experiments for various methanol fractions, it is shown that a fast retention was followed by a change to a more gradual release process that was slower and linear versus $t^{1/2}$. The abruptness of the transition between the two phases suggested a biphasic behavior. Linearity of cyprodinil retention onto soil versus $t^{1/2}$ indicates time intervals where soil cyprodinil content is controlled by diffusion. However, the existence of different time phases implies that a model with a constant diffusion coefficient is not valid for describing the whole process.

Release Dynamics. In each experiment, more than 95% of adsorbed cyprodinil was eluted during the release stage by passage of 45 reactor volumes of cyprodinil-free influent. The adsorption processes may be regarded as reversible. As during retention, during release it was possible to distinguish fast and slow processes, although in this case the transition from one to the other was more gradual (**Figure 4**).

Crank (22) shows that when diffusion is dependent on concentration there is a deviation in the linear behavior of the diffusion-controlled processes versus $t^{1/2}$. In this situation, the diffusion process is also controlled by the retardation coefficient, $R(c)$, which in turn depends on the concentration at equilibrium according to Freundlich's isotherms.

Modeling. In **Figure 5**, symbols represent the evolution with time of cyprodinil retention relative to the maximum capacity of its adsorption at equilibrium (q/q_e). It is observed that methanol causes an apparent increase in the velocity and relative efficiency of retention of cyprodinil on soil.

Accepting the role of diffusion in cyprodinil retention processes, we are able to obtain estimations of the effective one-dimensional diffusion coefficient, D_e' , from the slope of the linear segments in **Figure 4**. D_e' takes into account effects of

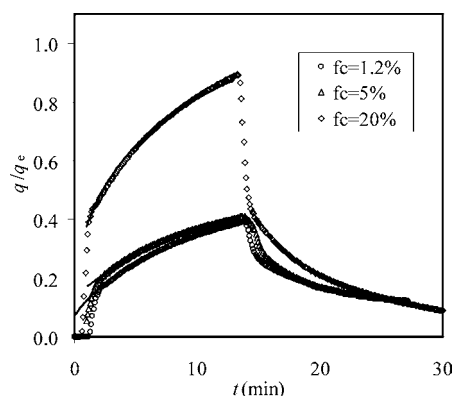


Figure 5. Dynamics of cyprodinil relative to the maximum capacity of its retention at equilibrium (q/q_e) for three concentrations of methanol, f_c . Lines along the slow retention phase show the best fittings obtained with the spherical diffusion model.

Table 3. Effective Diffusion Coefficients Characterizing the Fast and Slow Cyprodinil Adsorption Processes in the Presence of Various Methanol Concentrations

f_c (%)	q_e (mg/kg)	R	D^* (mg kg ⁻¹ min ^{-1/2})	$(D^*/q_e)^2$ (min ⁻¹)	$D_e' = (D^*/q_e)^2 L^2 R$ (cm ² min ⁻¹)	r^2
Fast Phase						
1.2	120	5.2	68.7	0.328	4.24×10^{-5}	0.992
5	85	4.4	38.1	0.201	2.21×10^{-5}	0.995
20	20	1.7	28.5	2.03	8.68×10^{-5}	0.996
Slow Phase						
1.2	12.3	5.2	68.7	0.0103	1.37×10^{-6}	0.997
5	7.9	4.4	38.1	0.0086	9.51×10^{-7}	0.994
20	4.4	1.7	28.5	0.0484	2.07×10^{-6}	0.997

Table 4. Estimation of the Fickian Coefficient of Intraparticle Diffusion (D_e) for the Slow Retention Phase According to the Spheric Diffusion Model of Crank (22) Considering both $L = 0.005$ cm and Linear Retention

f_c (%)	$D_R = D_e/R$ (cm ² min ⁻¹)	R	D_e (cm ² min ⁻¹)	r^2
1.2	3.20×10^{-8}	5.2	1.66×10^{-7}	0.994
5	5.44×10^{-8}	4.4	2.39×10^{-7}	0.988
20	1.96×10^{-7}	1.7	3.33×10^{-7}	0.999

intraparticle tortuosity. We therefore expect D_e' to be lower than the diffusion coefficient in the liquid phase. The equation of the diffusion model allows us to approximate D_e' for the geometric mean of the particle radius of the soil in the chamber ($L = 0.005$ cm), using the equivalent "linear" retardation factor $R = 1 + m/V_e K_{dc}$. **Table 3** shows the D_e' characterizing the fast and slow cyprodinil retention processes in the presence of various methanol concentrations.

Crank (22) derived solutions for diffusion in a sphere for later stages of the process. The relative concentration in the sphere for time t is given by

$$q(t)/q_e = 1 - 6/\pi^2 \sum_{j=1}^{\infty} j^{-2} \exp(-D_R j^2 \pi^2 t L^{-2}) \quad (5)$$

where j is a positive integer (from 1 to 10) and all other parameters are defined above. We optimized D_R from eq 5 to obtain the best estimations of $q(t)$ (**Table 4**) in the slow phase of retention (that corresponds to the late stage of the process). The calculated retention, represented by solid lines in **Figure 5**, shows that the linear retardation and diffusion model in spherical particles can describe partially the dynamics of retention.

Numerical Solution. The behavior of a complex system like this can be only partially understood if we do not use a model including nonlinear equilibrium sorption. For this reason, we have adopted a model based on the following three hypotheses. The diffusive transport process of solutes into soil particles consists of (i) transport from the bulk solution to the particle surface and across the boundary layer, (ii) micropore diffusion, and (iii) adsorption to external and internal surfaces. The boundary layer resistance depends on the efficiency of the stirring; ideal stirring causes the uptake rate to be controlled by diffusion through pores. The kinetic data $q(t)$ were modeled using a pore diffusion model incorporating the three time-dependent steps described above, the last including Freundlich's equation for nonlinear adsorption.

In ref 22, Crank sets out a general theory of one-dimensional diffusion in slabs, hollow cylinders, and spherical shells when D_e is a separable function of concentration and the space coordinates. For the flow through a spherical shell, the equation can be written as

$$\partial c/\partial t + m/V_e \partial q/\partial t = D_e(\partial^2 c/\partial l^2 + 2/l \partial c/\partial l) \quad (6)$$

Initially, we assumed a kinetic controlled sorption [$m/V_e (\partial q/\partial t)$]; therefore, the solution is defined by the appropriate system of equations of diffusion and adsorption. The initial conditions are as follows: $c = 0$ and $q = 0$ ($t = 0, 0 \leq l \leq L$). We assume that the bulk resistance by a rate of exchange is directly proportional to the difference between the actual concentration, $c_L(t)$, at the particle surface at any time and the average concentration in the external bulk solution, $c(t)$, which would be the result of the injection and mixing in the stirred-flow chamber. Mathematically, this means that the boundary condition at the particle surface is

$$D_e \partial c/\partial l = k_b[c(t) - c_L(t)] \text{ at } l = L \quad (7)$$

where k_b is a constant of proportionality that accounts for the linear transfer rate through the boundary layer and $c(t)$ is given by the equation of the stirred-flow reactor (eq 3). At the center of the particle, the boundary condition is

$$D_e \partial c/\partial l = 0 \text{ at } l = 0 \quad (8)$$

Equation 6, together with the surface sorption kinetics [$m/V_e (\partial q/\partial t)$], was numerically solved using the implicit, unconditionally stable Crank–Nicholson finite difference approximation with the MatLab 6 computer package (Mathworks, Inc., Natick, MA). The parameters were fitted to the experimental $q(t)$ data using a nonlinear least-squares minimization routine implemented in the model. We tested several initial assumptions for the parameters to fit in the search of the uniqueness of the fitted values. Particle radius was chosen as the geometric mean particle radius ($L = 0.005$ cm) calculated from the particle size distribution of the soil in the chamber.

Data in **Figure 4** were initially fitted with D_e , k_1 , and k_b as the fitting parameters. In all cases, the best kinetic adsorption model was a second-order model in which $dq/dt = k_1 c(K_{FC}^n - q)$ (data not shown). However, the fit of second-order constant k_1 tended to very high values ($k_1 > 10^4$) with standard errors of $> 100\%$. Given the actual conditions of the stirred-flow system, the local equilibrium of adsorption can be assumed from $k_1 > 10^2$. Thus, the expression of eq 6 was simplified for describing the local equilibrium adsorption as

$$\partial c/\partial t = D_e/R(c)(\partial^2 c/\partial l^2 + 2/l \partial c/\partial l) \quad (9)$$

Table 5. Fitted Intraparticle Transport Parameters (D_e and k_b) Using Experimental Isotherm Parameters and Nonlinear Retention (r^2 corresponds to only the retention stage)^a

f_c (%)	D_e (cm ² min ⁻¹)	k_b (cm/min)	r^2
1.2	1.62×10^{-7}	0.078	0.9045
5	1.08×10^{-7}	0.072	0.7041
20	5.59×10^{-7}	0.029	0.9610

^a The standard errors of the fitted parameters were $< 5\%$.

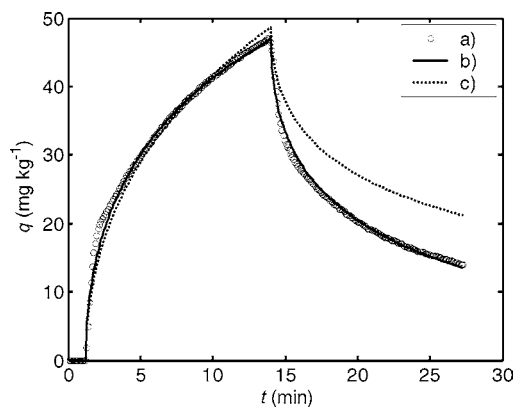


Figure 6. Dynamics of cyprodinil with an f_c of 1.2%: (a) experimental data from CSTR, (b) diffusion and nonlinear equilibrium adsorption model after fitting D_e , k_b , and Freundlich parameters (K_F and n), and (c) model using fitted D_e and k_b , together with experimental Freundlich parameters from batch experiments.

where $R(c) = 1 + m/V_e n K_{FC}^{n-1}$ is the nonlinear retardation factor in which $n K_{FC}^{n-1}$ is the first derivative of Freundlich's isotherm. Equation 9 together with $R(c)$ was then solved numerically, using the same procedure that was used for eq 8, with the same initial conditions for c . The boundary conditions were

$$D_e/R(c) \partial c/\partial l = k_b[c(t) - c_L] \text{ at } l = L \quad (10)$$

$$D_e/R(c) \partial c/\partial l = 0 \text{ at } l = 0 \quad (11)$$

The average adsorbed concentration in the soil particles for each time can be calculated from

$$q(t) = 3L^{-3} \int_{l=0}^{l=L} K_{FC} c(t, l)^n l^2 dl \quad (12)$$

The integral in eq 12 was solved numerically using the trapezoidal rule for each sampling time. We assumed that the dissolved mass of cyprodinil in the intraparticle pores can be neglected.

Modeling Results. The equilibrium adsorption model gave better results than the kinetic adsorption model. The best fitting values of D_e in the numerical approximation (**Table 5**) were greater than those shown in **Table 4**. These differences occurred because the numerical approximation was used to estimate D_e over the entire range of the retention stage and including the nonlinear $R(c)$.

The observed biphasic behavior was reproduced by the model and is related to the nonlinearity of the adsorption isotherm (**Figures 6–8**). “Extra steepness” at initial stages of retention and release cannot be explained by the nonlinear isotherm. We suggest that this extra steepness was caused by adsorption of cyprodinil on the smallest particles (i.e., clay size and colloids) and the external rough surfaces of greater particles. In these

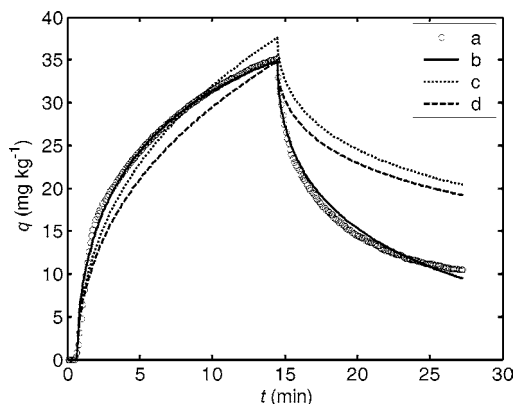


Figure 7. Dynamics of cyprodinil with an f_c of 5%: (a) experimental data from CSTR, (b) diffusion and nonlinear equilibrium adsorption model after fitting D_e , k_b , and Freundlich parameters (K_F and n), and (c and d) the two best fittings of D_e and k_b using the experimental Freundlich isotherm parameters obtained from batch experiments.

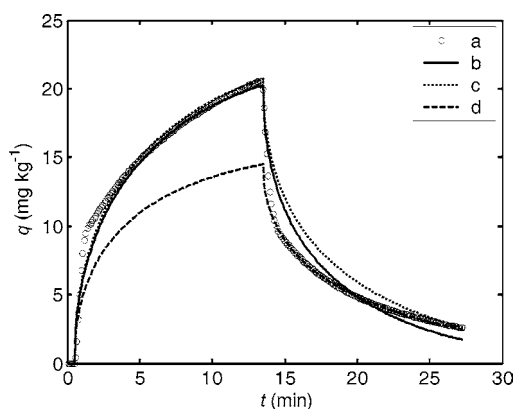


Figure 8. Dynamics of cyprodinil with an f_c of 20%: (a) experimental data from CSTR, (b) diffusion and nonlinear equilibrium adsorption model after fitting D_e , k_b , and Freundlich parameters (K_F and n), (c) best fittings of D_e and k_b using the experimental Freundlich isotherm parameters obtained from batch experiments, and (d) fitting D_e , k_b , K_F , and n for the release stage only.

situations, diffusion is less limiting; therefore, a faster retention could be expected at early times with respect to a theoretical sphere.

A salient finding is the apparent hysteresis of the retention and release, which can be seen in the figures. Using experimental values of K_F and n , together with fitted values of D_e and k_b in the model (Table 5), it was found that the release is underestimated with respect to the experimental data (see dotted lines in Figures 6–8). The fitted K_F values in the release time segment were smaller than their corresponding values in the retention stage. This hysteresis behavior was the opposite of that expected in the batch experiments.

Table 6 shows the best fitting values of K_F , n , D_e , and k_b that describe the two consecutive retention–release stages (solid lines in Figures 6–8). Fitted K_F values were smaller than those obtained from batch experiments for all f_c values, indicating that in the kinetic experiments the retention was weaker than that expected in the batch tests. We interpret that on a shorter time scale (30') only the equilibrium and reversible sorption are revealed as the dominant mechanisms. In batch equilibrium experiments, the greater adsorption suggests the existence of slower adsorption processes contributing to the total adsorption capacity.

Table 6. Fitted Intraparticle Transport Parameters (D_e and k_b) and Fitted Isotherm Parameters (K_F and n) for Retention and Release Stages^a

f_c (%)	D_e ($\text{cm}^2 \text{min}^{-1}$)	k_b (cm/min)	K_F ($\text{mg}^{1-n} \text{kg}^{-1} \text{L}^n$)	n	r^2
1.2	5.58×10^{-7}	0.058	21.9	0.84	0.9961
5	6.52×10^{-7}	0.062	13.6	0.68	0.9948
20	7.27×10^{-7}	0.026	5.96	0.91	0.9945

^a The standard errors of the fitted parameters were <8% except for n (<11%).

The most important effect of methanol on the cyprodinil retention–release dynamics is due to changes in the equilibrium of adsorption. The effect of methanol also increased D_e and decreased k_b (Table 6); these results suggested greater mobility of cyprodinil in the intraparticle pores and a diminution of the gradient driving force.

The salient findings of this study are as follows. (1) The effective partition constant for the partitioning of cyprodinil between the studied soil and mixtures of methanol and aqueous CaCl_2 , K_{dc} , decreases linearly with an increase in methanol fraction f_c up to 20%. (2) The dynamics of retention of cyprodinil on the studied soil from such mixtures is controlled by diffusion, while the surface adsorption is described well by a nonlinear equilibrium isotherm. (3) The sorption of cyprodinil from the studied soil into these media is reversible, and the major effect on the kinetics is due to the changes in the affinity between the soil and methanol. (4) The Freundlich isotherm parameters obtained from batch equilibrium were larger than those obtained from kinetic experiments.

NOMENCLATURE

c (mg/L)	concentration of cyprodinil in the liquid phase
$c(t)$ (mg/L)	average c at time t
c_i (mg/L)	concentration of cyprodinil in the liquid phase of the reactor and the effluent at discrete time step i
c_e (mg/L)	concentration of cyprodinil in solution at equilibrium
c_{in} (mg/L)	concentration of cyprodinil in the influent
$c(t,l)$	c at time t in the particle domain ($0 < l < L$)
D^* ($\text{mg kg}^{-1} \text{min}^{-1/2}$)	slope of the linear relation q versus $t^{1/2}$
D_R ($\text{cm}^2 \text{min}^{-1}$)	linearly retarded coefficient of diffusion
D_e' ($\text{cm}^2 \text{min}^{-1}$)	estimated effective one-dimensional Fickian coefficient of diffusion, including the effect of the tortuosity of micropore paths
D_e ($\text{cm}^2 \text{min}^{-1}$)	effective Fickian coefficient of diffusion (for spherical geometry)
f_c (vol %)	methanol concentration
J (L/min)	flow rate
k_b (cm/min)	coefficient of the mass transfer at the solid–liquid interface
K_{dc} (L/kg)	partition coefficient between the soil and cosolvent (methanol/water)
K_{dw} (L/kg)	K_{dc} for a zero methanol concentration
K_F ($\text{mg}^{1-n} \text{kg}^{-1} \text{L}^n$)	pre-exponential factor of Freundlich's isotherm
L (cm)	radius of the soil particle

l (cm)	distance from the center of the particle to the surface
m (kg)	mass of soil in the reactor
n	Freundlich's exponent
q (mg/kg)	amount of cyprodinil retained in the soil
$q(t)$ (mg/kg)	average q at time t
q_e (mg/kg)	amount of cyprodinil sorbed in soil at equilibrium
$R(c)$	nonlinear retardation function $(1 + m/V_e dq/dc)$
R	linear retardation factor $R(1 + m/V_e K_{dc})$
t (min)	time
V_e (L)	effective volume of solution in the reactor

LITERATURE CITED

- Iraqi, S. M. U.; Iraqi, E. Sorption of the pesticide endosulphan on two Indian soils. *J. Colloid Interface Sci.* **2000**, *224*, 155–161.
- Lee, L. S.; Bellin, C. A.; Pinal, R.; Rao, P. S. C. Cosolvent effects on sorption of organic acids by soils from mixed solvents. *Environ. Sci. Technol.* **1993**, *27*, 165–171.
- Sanchez-Camazano, M.; Arienzo, M.; Sanchez-Martin, M. J.; Crisanto, T. Effect of different surfactants on the mobility of selected non-ionic pesticides in soil. *Chemosphere* **1995**, *31*, 3793–3801.
- Wood, A.; Bouchard, D. C.; Brusseau, M. L.; Rao, P. S. C. Cosolvent effects on sorption and mobility of organic contaminants in soils. *Chemosphere* **1990**, *21*, 575–587.
- Brusseau, M. L.; Wood, A. L.; Rao, P. S. C. Influence of organic cosolvents on the sorption kinetics of hydrophobic organic chemicals. *Environ. Sci. Technol.* **1991**, *25*, 903–910.
- Rao, P. S. C.; Hornsby, A. G.; Kilcrease, D. P.; Nkedi-Kizza, P. Sorption and transport of hydrophobic organic chemicals in aqueous and mixed solvent systems: Model development and preliminary evaluation. *J. Environ. Qual.* **1985**, *14*, 376–383.
- Arienzo, M.; Sanchez-Camazano, M.; Crisanto-Herrero, T.; Sanchez-Martin, M. J. Effect of organic cosolvents on adsorption of organophosphorus pesticides by soils. *Chemosphere* **1993**, *27*, 1409–1417.
- Bouchard, D. C. Sorption kinetics of PAHs in methanol–water systems. *J. Contam. Hydrol.* **1998**, *34*, 107–120.
- Haws, N. W.; Ball, W. P.; Brower, E. J. Modeling and interpreting bioavailability of organic contaminant mixtures in subsurface environments. *J. Contam. Hydrol.* **2006**, *82*, 255–292.
- He, Y.; Li, P.; Yalkowsky, S. H. Solubilization of Fluasterone in cosolvent/cyclodextrin combinations. *Int. J. Pharm.* **2003**, *264*, 25–34.
- Bar-Tal, A.; Sparks, D. L.; Peseck, J. D.; Feigenbaum, S. Analyses of adsorption kinetics using a stirred-flow chamber: I. theory and critical tests. *Soil Sci. Soc. Am. J.* **1990**, *54*, 1273–1278.
- Carski, T. H.; Sparks, D. L. A modified miscible displacement technique for investigating adsorption–desorption kinetics in soils. *Soil Sci. Soc. Am. J.* **1985**, *49*, 1114–1116.
- Shi, Z.; Di Toro, D. M.; Allen, H. E.; Ponizovsky, A. A. Modeling kinetics of Cu and Zn release from soils. *Environ. Sci. Technol.* **2005**, *39*, 4562–4568.
- Heyse, E.; Dai, D.; Rao, P. S. C.; Delfino, J. J. Development of a continuously stirred flow cell for investigating sorption mass transfer. *J. Contam. Hydrol.* **1997**, *25*, 337–355.
- de Jonge, H.; Heimovaara, T.; Verstraten, J. Naphthalene sorption to organic soil materials studied with continuous stirred flow experiments. *Soil Sci. Soc. Am. J.* **1999**, *63*, 297–306.
- Rial Otero, R.; Cancho Grande, B.; Arias Estevez, M.; Lopez Periago, E.; Simal Gandara, J. Procedure for the measurement of soil inputs of plant-protection agents washed off through vineyard canopy by rainfall. *J. Agric. Food Chem.* **2003**, *51*, 5041–5046.
- JMPR. Pesticide residues in Food–2003: Report of the Joint Meeting of the FAO Panel of Experts on Pesticide Residues in Food and the Environment and the WHO Core Assessment Group on Pesticide Residues, Geneva, Switzerland, Sept 15–24, 2003; WHO and FAO: Rome, 2004; pp 169–287.
- Arias, M.; Torrente, A. C.; Lopez, E.; Soto, B.; Simal-Gandara, J. Adsorption–desorption dynamics of cyprodinil and fludioxonil in vineyard soils. *J. Agric. Food Chem.* **2005**, *53*, 5675–5681.
- Soil Survey Staff. *Keys to soil taxonomy*; Pocahontas Press: Blacksburg, VA, 1997.
- Strawn, D. G.; Sparks, D. L. Effects of soil organic matter on the kinetics and mechanisms of Pb(II) sorption and desorption. *Soil Sci. Soc. Am. J.* **2000**, *64*, 144–146.
- Yin, Y.; Allen, H. E.; Huang, C. P.; Sparks, D. L.; Sanders, P. F. Kinetics of mercury(II) adsorption and desorption on soil. *Environ. Sci. Technol.* **1997**, *31*, 496–503.
- Crank, J. *The Mathematics of Diffusion*, 2nd ed.; University Press: Oxford, U.K., 1975.

Received for review December 14, 2005. Revised manuscript received May 8, 2006. Accepted May 9, 2006. Funds from Xunta de Galicia (Autonomous Community Government in Northwest Spain, PGIDIT03PXIB38302PR) and from the Spanish Ministry of Science and Technology (AGL2003-02244) are acknowledged. This work was also funded through Ramón y Cajal research contracts awarded to M.A.-E. and J.E.L.-P.

JF053128E